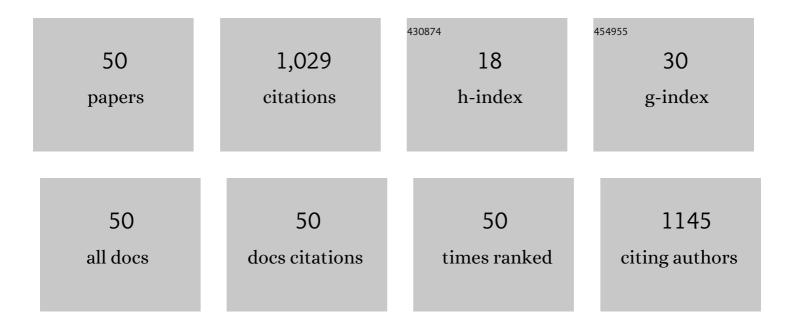
Yong-Tao Li

List of Publications by Year in descending order

Source: https://exaly.com/author-pdf/8016606/publications.pdf Version: 2024-02-01



YONG-TAO LL

#	Article	IF	CITATIONS
1	Reversible room temperature hydrogen storage in high-entropy alloy TiZrCrMnFeNi. Scripta Materialia, 2020, 178, 387-390.	5.2	132
2	Hydrogen-induced magnesium–zirconium interfacial coupling: enabling fast hydrogen sorption at lower temperatures. Journal of Materials Chemistry A, 2017, 5, 5067-5076.	10.3	94
3	Enhanced reducibility and redox stability of Fe ₂ O ₃ in the presence of CeO ₂ nanoparticles. RSC Advances, 2014, 4, 47191-47199.	3.6	70
4	Mechanical Synthesis and Hydrogen Storage Characterization of MgVCr and MgVTiCrFe Highâ€Entropy Alloy. Advanced Engineering Materials, 2020, 22, 1901079.	3.5	54
5	Enhancing hydrogen sorption in MgH2 by controlling particle size and contact of Ni catalysts. Rare Metals, 2021, 40, 995-1002.	7.1	43
6	In situ forming LiF nanodecorated electrolyte/electrode interfaces for stable all-solid-state batteries. Materials Today Nano, 2020, 10, 100079.	4.6	38
7	Potassium octahydridotriborate: diverse polymorphism in a potential hydrogen storage material and potassium ion conductor. Dalton Transactions, 2019, 48, 8872-8881.	3.3	34
8	<i>In Situ</i> Embedding of Mg ₂ NiH ₄ and YH ₃ Nanoparticles into Bimetallic Hydride NaMgH ₃ to Inhibit Phase Segregation for Enhanced Hydrogen Storage. Journal of Physical Chemistry C, 2014, 118, 23635-23644.	3.1	33
9	Comparative Investigations on Hydrogen Absorption–Desorption Properties of Sm–Mg–Ni Compounds: The Effect of [SmNi5]/[SmMgNi4] Unit Ratio. Journal of Physical Chemistry C, 2015, 119, 4719-4727.	3.1	33
10	Carbon nanomaterial-assisted morphological tuning for thermodynamic and kinetic destabilization in sodium alanates. Journal of Materials Chemistry A, 2013, 1, 5238.	10.3	30
11	Enhancement of Hydrogen Storage in Destabilized LiNH ₂ with KMgH ₃ by Quick Conveyance of N-Containing Species. Journal of Physical Chemistry C, 2016, 120, 1415-1420.	3.1	28
12	Ultra-Fine CeO ₂ Particles Triggered Strong Interaction with LaFeO ₃ Framework for Total and Preferential CO Oxidation. ACS Applied Materials & Interfaces, 2020, 12, 42274-42284.	8.0	24
13	Enhanced dehydrogenation of ammonia borane by reaction with alkaline earth metal chlorides. International Journal of Hydrogen Energy, 2012, 37, 4274-4279.	7.1	20
14	Facile preparation of carbon-coated Mg nanocapsules as light microwave absorber. Materials Letters, 2015, 149, 12-14.	2.6	20
15	Self-Printing on Graphitic Nanosheets with Metal Borohydride Nanodots for Hydrogen Storage. Scientific Reports, 2016, 6, 31144.	3.3	20
16	Hydrogen storage properties of TiMn1.5V0.2-based alloys for application to fuel cell system. Journal of Power Sources, 2010, 195, 8215-8221.	7.8	19
17	Improved dehydrogenation of TiF ₃ -doped NaAlH ₄ using ordered mesoporous SiO ₂ as a codopant. Journal of Materials Research, 2010, 25, 2047-2053.	2.6	19
18	Facile self-assembly of light metal borohydrides with controllable nanostructures. RSC Advances, 2014, 4, 983-986.	3.6	19

Yong-Tao Li

#	Article	IF	CITATIONS
19	Solid solution of Cu in Mg2NiH4 and its destabilized effect on hydrogen desorption. Materials Chemistry and Physics, 2017, 193, 1-6.	4.0	19
20	Improving the phase stability and cycling performance of Ce ₂ Ni ₇ -type RE–Mg–Ni alloy electrodes by high electronegativity element substitution. Dalton Transactions, 2018, 47, 16453-16460.	3.3	19
21	Boosting Photovoltaic Performance and Stability of Super-Halogen-Substituted Perovskite Solar Cells by Simultaneous Methylammonium Immobilization and Vacancy Compensation. ACS Applied Materials & Interfaces, 2020, 12, 8249-8259.	8.0	19
22	Hydrogen storage of a novel combined system of LiNH ₂ –NaMgH ₃ : synergistic effects of in situ formed alkali and alkaline-earth metal hydrides. Dalton Transactions, 2013, 42, 1810-1819.	3.3	17
23	Fast hydrogen-induced optical and electrical transitions of Mg and Mg-Ni films with amorphous structure. Applied Physics Letters, 2013, 102, .	3.3	17
24	Crystallite growth characteristics of Mg during hydrogen desorption of MgH2. Progress in Natural Science: Materials International, 2020, 30, 246-250.	4.4	17
25	Activity-Tuning of Supported Co–Ni Nanocatalysts via Composition and Morphology for Hydrogen Storage in MgH2. Frontiers in Chemistry, 2019, 7, 937.	3.6	17
26	<scp>Anionâ€Regulated Weakly Solvating</scp> Electrolytes for <scp>Highâ€Voltage</scp> Lithium Metal Batteries. Energy and Environmental Materials, 2023, 6, .	12.8	17
27	Enhanced hydrogen storage kinetics of an Mg–Pr–Al composite by in situ formed Pr3Al11 nanoparticles. Dalton Transactions, 2019, 48, 7735-7742.	3.3	15
28	Transformation and superelastic characteristics of large hysteresis TiNi matrix shape memory alloys reinforced by V nanowires. Materials Letters, 2018, 228, 391-394.	2.6	14
29	Turning bulk materials into 0D, 1D and 2D metallic nanomaterials by selective aqueous corrosion. Chemical Communications, 2019, 55, 10476-10479.	4.1	12
30	Effect of plastic deformation of V nanowires on the transformation characteristics of NiTiV alloys. Materials Science & Engineering A: Structural Materials: Properties, Microstructure and Processing, 2018, 735, 162-165.	5.6	11
31	Intrinsic alterations in the hydrogen desorption of Mg ₂ NiH ₄ by solid dissolution of titanium. Dalton Transactions, 2018, 47, 8418-8426.	3.3	11
32	Controlled phase evolution from Cu _{0.33} Co _{0.67} S ₂ to Cu ₃ Co ₆ S ₈ hexagonal nanosheets as oxygen evolution reaction catalysts. RSC Advances, 2019, 9, 9729-9736.	3.6	11
33	Enhanced Low-Temperature Hydrogen Storage in Nanoporous Ni-Based Alloy Supported LiBH4. Frontiers in Chemistry, 2020, 8, 283.	3.6	10
34	Carbon/Sulfur Composites Stabilized with Nano-TiNi for High-Performance Li–S Battery Cathodes. ACS Applied Energy Materials, 2019, 2, 1537-1543.	5.1	9
35	A systematic computational investigation of the water splitting and N ₂ reduction reaction performances of monolayer MBenes. Physical Chemistry Chemical Physics, 2021, 23, 6613-6622.	2.8	9
36	Interface controlled solid-state lithium storage performance in free-standing bismuth nanosheets. Dalton Transactions, 2021, 50, 252-261.	3.3	8

Yong-Tao Li

#	Article	IF	CITATIONS
37	Uniform gallium oxyhydroxide nanorod anodes with superior lithium-ion storage. RSC Advances, 2019, 9, 34896-34901.	3.6	7
38	Effect of cold work on martensitic transformation of Ni38Ti37V25 alloy reinforced by V nanowires. Journal of Alloys and Compounds, 2020, 815, 152489.	5.5	7
39	Pressure hysteresis in the TiMn _{1.5} V <i>_x</i> -H ₂ (<i>x</i> = 0.1–0.5) system. Journal of Materials Research, 2009, 24, 2886-2891.	2.6	5
40	Enhancement of the ionic conductivity of lithium borohydride by silica supports. Dalton Transactions, 2021, 50, 15352-15358.	3.3	5
41	Fabrication of GeS-graphene composites for electrode materials in lithium-ion batteries. Materials Research Express, 2021, 8, 115013.	1.6	5
42	Promoted hydrogen release from 3LiBH4/MnF2 composite by doping LiNH2: Elimination of diborane release and reduction of decomposition temperature. International Journal of Hydrogen Energy, 2012, 37, 18074-18079.	7.1	4
43	Effect of Microstructure on Hydrogen Permeation in EA4T and 30CrNiMoV12 Railway Axle Steels. Metals, 2019, 9, 164.	2.3	4
44	The superior desorption properties of MgCl ₂ -added ammonia borane compared to MgF ₂ -added systems—the unexpected role of MgCl ₂ interacting with [NH ₃] units. RSC Advances, 2017, 7, 36684-36687.	3.6	3
45	The transformation characteristics of the NiTi–V composite with dual-scale bcc-V fibers. Intermetallics, 2020, 116, 106650.	3.9	3
46	Effects of morphology of V nanowires on superelasticity of Ti46Ni44V10 alloy. Materials Science & Engineering A: Structural Materials: Properties, Microstructure and Processing, 2020, 786, 139450.	5.6	2
47	Phase component and microstructure of laser-sintered Mg-Ni alloys. Rare Metals, 2008, 27, 400-404.	7.1	1
48	Hydrogen Storage Properties and Reactive Mechanism of LiBH4/Mg10YNi-H Composite. Materials Research, 2019, 22, .	1.3	1
49	Direct mechanochemical formation of alkali metal borohydrides nanocrystals exhibiting kinetic and thermodynamic destabilizations. International Journal of Hydrogen Energy, 2016, 41, 2807-2813.	7.1	0
50	Thermal Dehydrogenation Characteristics of Li-Sr-Al-N-H Hydrogen Storage System. Materials Research, 2018, 21, .	1.3	0